Aerodynamics of a circular planform wing

Aerodynamics of a circular planform wing

Suliman M. M. Ali[1], Ashraf A. Omar[2], Waleed Fekry faris[3], Ahmad Faris Ismail[4], J. S. Mohamed Ali[5]

Kulliyyah of Engineering, International Islamic University Malaysia

waleed@iium.edu.my

Abstract. This paper investigates the aerodynamics of a circular plan form wing at high Reynolds numbers numerically. Commercial software STAR-CCM+ has been used for the study. The numerical results were presented in terms of flow visualization, pressure over the wing, velocity contour and streamlines, lift and drag coefficients for angle of attacks ranging from 0˚ to 30˚ and Reynolds number equal to 510,000. The results showed that the distribution of the pressure is dominated by vortices behaviour at high angle of attack. The results also show that there is a large separation region located on the trailing edge of the elevator and the cockpit region. It is evident that this type of wing configurations plays a very important role in delaying or preventing the flow separation. The result agreed with available experimental data.
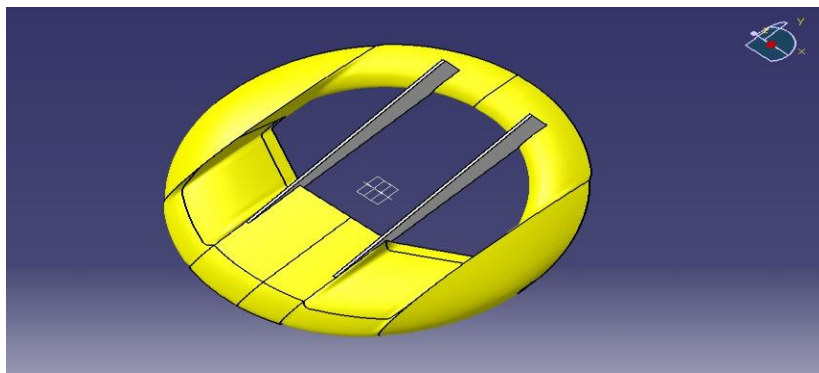
1. Introduction

Aircraft with low aspect ratio wings behave differently than high aspect ratio aircraft, such as the USAF B52 bomber and sail planes. A larger taper will lead to more unstable characteristics when compared to a low tapered wing with a high aspect ratio. Dating back to the early 1940's, several disk shaped aircraft were constructed and tested for both personal and military applications. Arthur Sack constructed a low aspect ratio circular planform aircraft [1]. During takeoff tests, it was noticed that the control surfaces were in a lower pressure area behind the circular wing.One of the most unusual aircraft ever designed for the U.S. Navy was the Chance Vought V-173, also known as the Zimmerman "Flying Pancake". It was a prototype "proof of concept" aircraft that lacked wings, instead relying on its flat circular body to provide the lifting surface [2]. As early as 1933, Charles Zimmerman had experimentally studied several airplanes with low aspect ratio wings and found a range of aspect ratios extending approximately from 0.75 to 1.50 [3].. He later determined from experiments that low aspect ratio wing designs were more efficient than conventional wings when the vortices from the wing were controlled with propellers [4].. One of the more interesting configurations tested was a military concept   the Lenticular Reentry Vehicle or LRV . This was studied in the 1960's. Its design was considered because it created more lift than a standard wing, especially at low speeds [4]. . After testing several configurations in wind tunnels at subsonic speeds, it was found that the optimal LRV produced longitudinal stability, a positive pitching moment at zero angle of attack and a maximum lift to drag ratio of five. In the early 1970s the U.S. Navy commissioned a project in which the aerodynamic characteristics of a self-suspended Frisbee shaped flare was investigated [5].. Both spinning and non-spinning models were tested and it was found that spin had negligible effects on the aerodynamic forces and moments. Later, Stilley and Carstens [5].. a circular palnform wing was studied, it was concluded that low sect ratio aircraft has more stability [6].

In the early 1970s the U.S. Navy commissioned a project in which the aerodynamic characteristics of a self-suspended Frisbee shaped flare was investigated [7]. Both spinning and non-spinning models were tested and it was found that spin had negligible effects on the aerodynamic forces and moments.

In August 9, 2008 two Geobat models had been tested in Auburn University's wind tunnel test [8]. In this paper, the numerical study of the flow around IIUM designed circular wing remote controlled aerial vehicle was carried out to study the aerodynamic performance of the circular wing configuration.

2. Study model

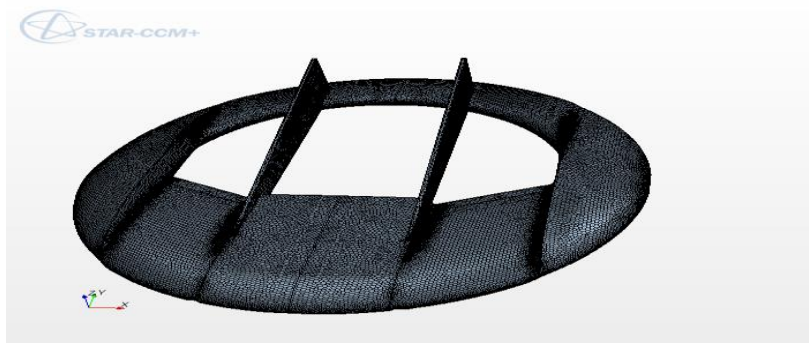

Figure 1. Circular wing geometry.

The studied models had a disk-shaped body of 0.72 m outer diameter with a central opening. The model can be described as a joined wing with a circular arc rearward swept front wing, a forward-swept rear wing with a circular trailing edge and two connecting wing tips, thus creating a 360 degree circular planform. The control surfaces included flaps, rear ailerons, a large elevator and two rudders. Each section of the wing was contoured with NACA 4412 airfoil geometry. The nominal thickness was 12% but was varied, decreasing slightly in thickness moving away from the centerline. Figure 1 shows a top schematic view of the circular wing. The wing geometry was created in CATIA, and later transformed into Initial Graphics Exchange Specification (IGES) file format. The neutral data format is imported to Star Design for preliminary setup. A computational grid of C-H type was generated from this boundary region. Sufficient spacing of 15 diameters between the wing model and the boundary region was selected. The boundary region was defined as free-stream control volume.

3. Meshing

The mesh was decided to generate using polyhedral cells along with prism layer mesh. Table 1 summarizes the overall mesh properties used to represent the model. As shown in Fig. 2., a very fine and high intensity mesh was created on the circular wing in order to preserve and to capture the details of the curvature of the surface as well as the intersection between wing and the domain.

Table 1: Mesh properties of scaled half-model of the circular wing.
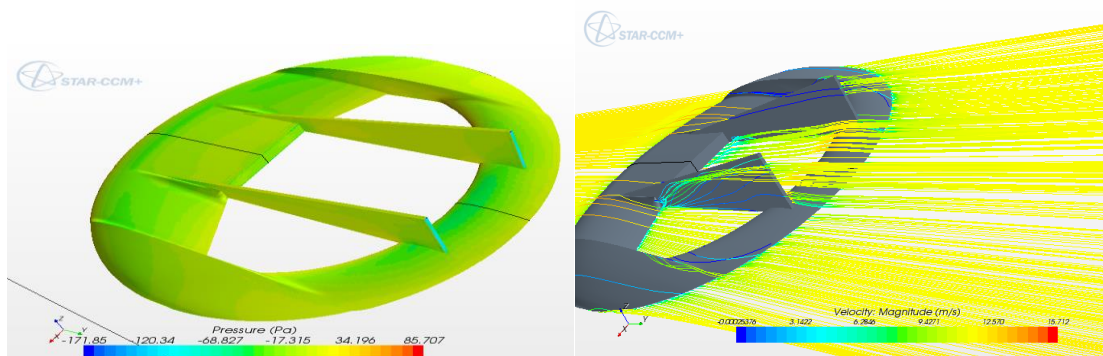
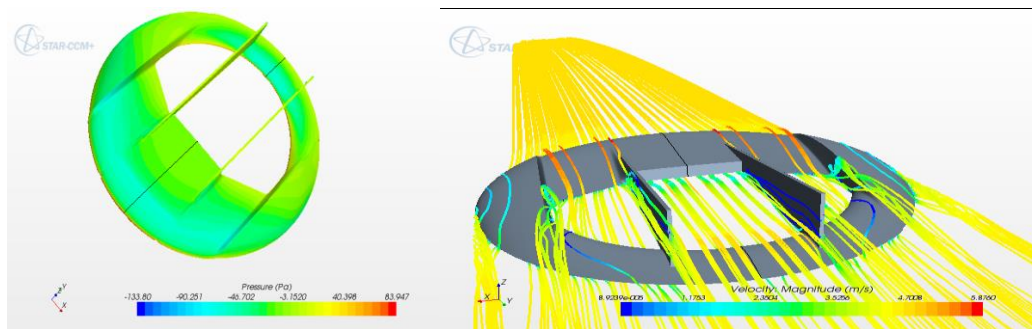| Mesh property	Parameter
Mesh type	Polyhedral mesher
Number of prism layers	15
Prism layer stretching	1.3%
Prism layer thickness	15 mm
Cell size (domain)	Max: 0.3 mm, Min: 0.075 mm
Cell size (Circular wing)	Max: 5 mm, Min: 1 mm
Growth rate	1.3%
Total number of cells	1145160

Figure 2. Surface mesh

4. Result and discussion

4.1. Flow visualization
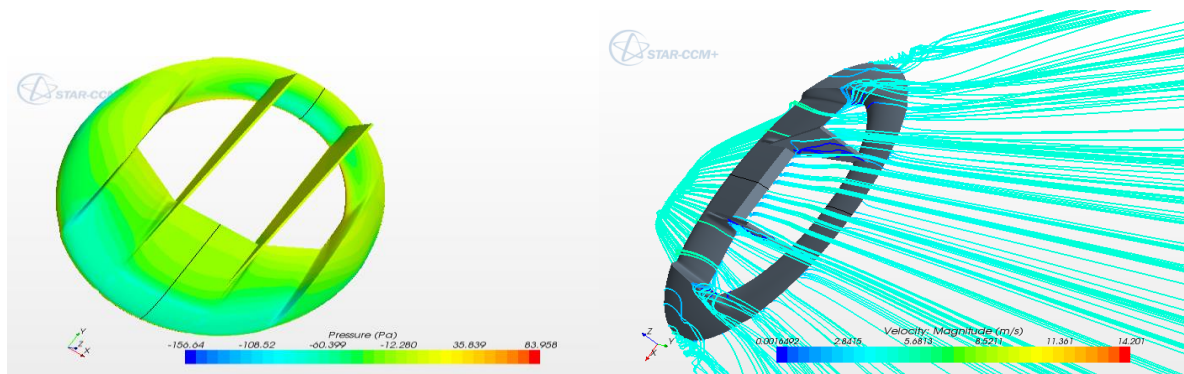
Flow visualization of the circular wing at different angles of attack is presented in Figures 3 to 6 for Reynolds number of 5.1×10^5. Fig. 3. reveals laminar attached flow with no separation bubble located on the model. There is a high pressure region located on the trailing edge of the elevator as well as separation region near the cockpit and with evident of the existing of detached flow with even more predominant pressure over the cockpit. The flow is completely laminar flow, this is could be the reason for the neutrally stability found in the pitching moment plots.

Figure 3. Pressure and streamlines over the circular wing at α = 0 deg.
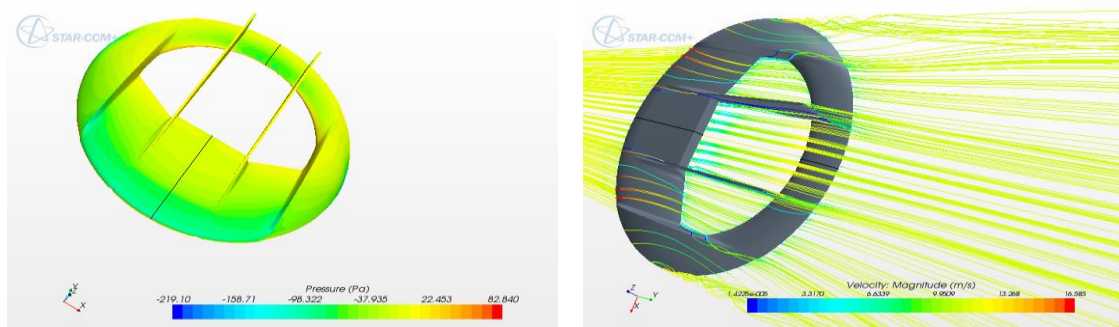
Figure 4. Pressure and streamlines over the circular wing = 10 deg

As the angle of attack is increased to 10 1nd 15 degrees, there is a noticeable change in the structure of the flow with the addition of the separation bubble on the leading edge of the wing. Figure 5 shows this trend but still yields the same pressure on the trailing edges of the control surfaces as well as separation on the top of the cockpit. As α is increased to 15 degrees, several different flow characteristics are observed. Figure 5 shows complete formation of the separation bubble span wise on the airfoil. Existence of a vortex can be seen more prominently at 20 degrees α as shown in Figure 6.

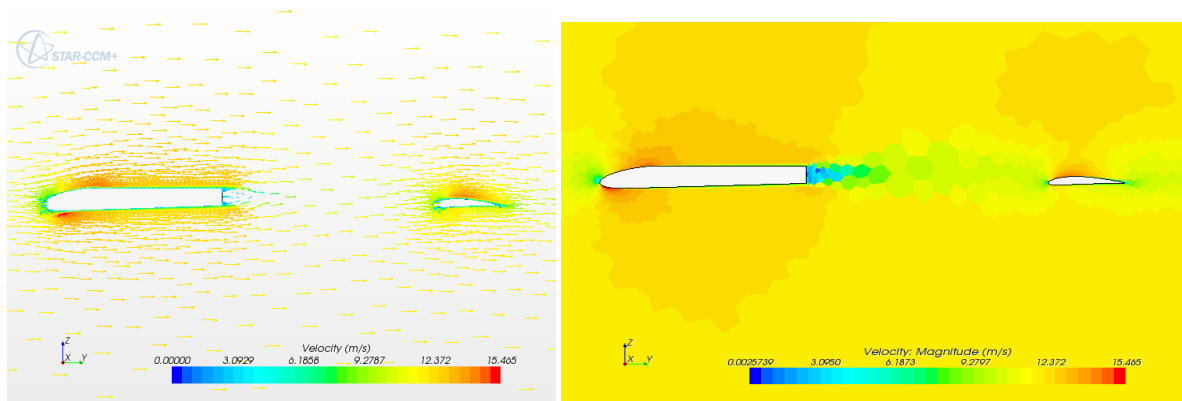

Figure 5. Pressure and streamlines over the circular wing at α = 15 deg.

A complete stall of the aircraft happened at an angle of attack of 27 degrees. Flow on the upper surface has completely changed direction and is moving towards the front of the aircraft.
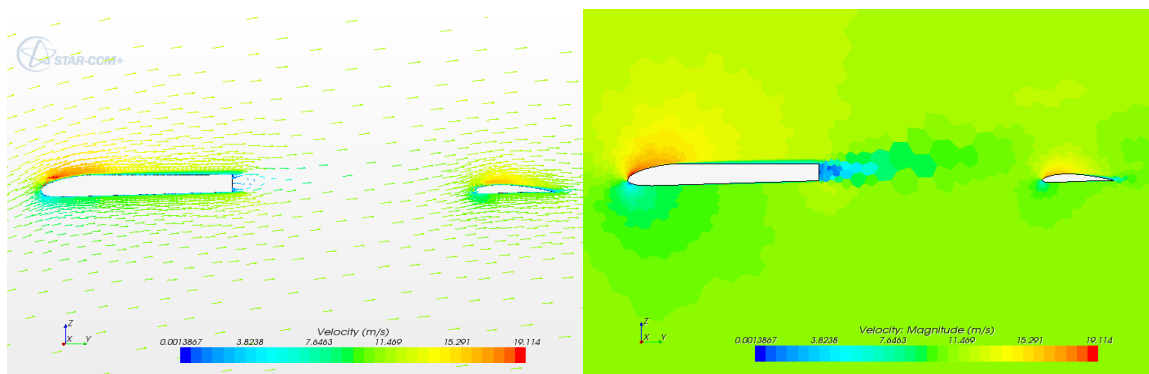

Figure 6. Pressure and streamlines over the circular wing at α = 20 deg

Figure 7. Velocity at y= 0.36m, α =0.

Reynolds number was set as turbulent, which is Re=5.1x10^5 with inflow velocity was set as 12 m/s. The results were performed for angle of attack ranged from 0 degree to 27 degree in order to reach stall angle. However, for this case, simulation was done for two assumptions were considered they are laminar and turbulent since Reynolds number presented transition Reynolds. It can be seen from figures 7 and 10 that the separation region is increased with increasing angle of attack. The separation regions are located at trailing and leading edge of wing.
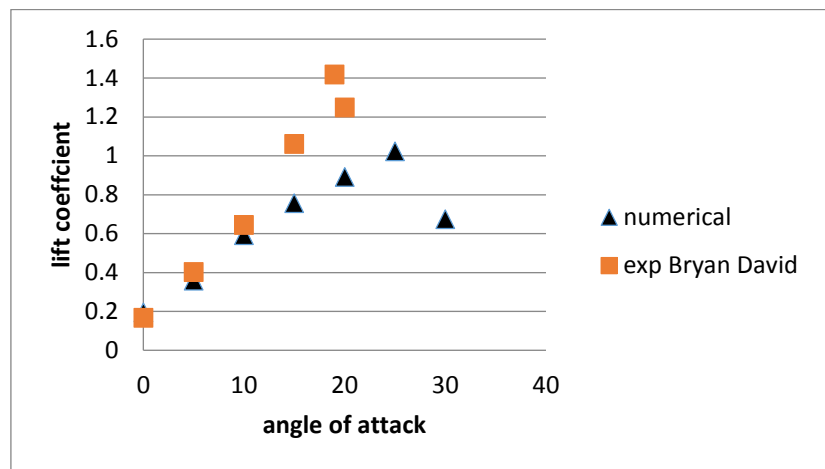

Figure 8. Velocity at y= 0.36m, α =25.

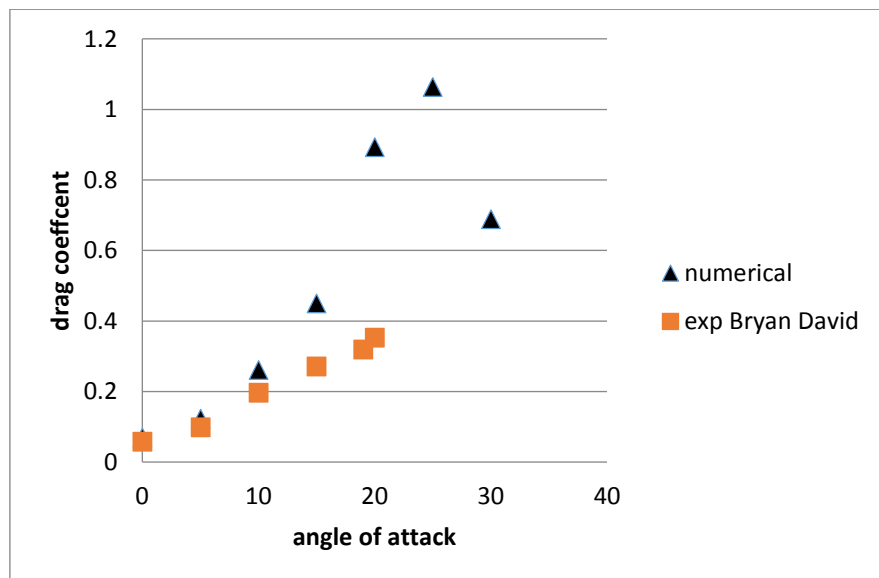*4.2. Aerodynamics coefficients*

Figures 9, 10 and 11 represent the aerodynamics force coefficients plot from numerical result for the wing with varies angle of attacks and viscous regime models. As seen from Figure 11, the lift curve slope is larger and has a good stall characteristic, which is at 27 degrees AOA. It also shows that as the lift coefficient increases, the drag coefficient also increases. In term of stability, the wing model can be classified as stable aircraft. Since the experimental testing that carried out by Bryan David (11) was difference Geometry, wing sections and speed but here we can compare the trend for the aerodynamics force coefficient curve distribution. Here, we will only compare the trend for Re=5.1x10^5 as the prototype that built by Recktenwald was tested at the same Reynolds number as this study. Hence, there is only dynamic similarity regardless of Geometric similarity. As shown in Figures 7 and 8, the trends for lift, drag and drag polar curve are almost identical. It was noticed that the wing model that used in this project has better characteristic for stall AOA. In term of stability, both prototype and the wing model share the same characteristic, which is they are statically stable aircrafts.
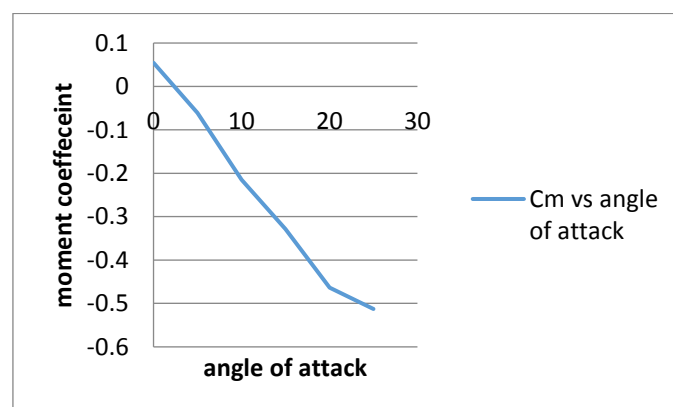
Figure 9. Lift vs angle of attack.

Figure 10. Drag vs angle of attack.

Figure 11. Moment coefficient vs angle of attack

5. Conclusion

This visualization results shown that the flow was already turbulent in nature. Additional flow structures observed on the circular wing cockpit, control surface trailing edge. The separation vortices increased with angle of attack. The experimental result has shown an agreement with a numerical result as it is clear in figures 3 to 11.

References
[1]   Anderson JD. 1999 Aircraft performance and design. *Vol. 1. WCB/McGraw-Hill Boston*, MA
[2]   Anderson Jr JD. 2010 *Fundamentals of aerodynamics. Tata McGraw-Hill Education.*
[3]   Von Kaenel R, Rizzi A, Oppelstrup J, Goetzendorf-Grabowski T, Ghoreyshi M, Cavagna. 2008 simulating stability & control with CFD/CSM in aircraft conceptual design. *In: 26th International Congress of the Aeronautical Sciences,* ICAS, pp. 14–9
[4]   Wilson T. 2008 *Americas Nuclear Flying Saucer*. Pop Mech.
[5]   Raymer DP, Zhang M, Rizzi AW, Raymer EN. 2017 Sparky Flapjack: Aircraft Design Inspirations from the Vought 173. *In: 55th AIAA Aerospace Sciences Meeting*, pp. 1184.
[6]   Suliman MM, Omar AA, Syed Mohamed Ali J. 2013 Flow visualization over a circular planform wing. *In: 2nd International Conference on Mechanical, Automotive and Aerospace Engineering (ICMAAE' 13), 2-4 July 2013, Kuala Lumpur, Malaysia.*
[7]   Stilley GD. 1972 Aerodynamic analysis of the self sustained flair. AD-740117, *Nav Ammunit Depot, Crane, Ind.*
[8]   Recktenwald B. 2008 Aerodynamic Testing of a Circular Planform Concept Aircraft.